Isotope and geochemical fingerprinting of placer gold: insights into the provenance and age

Svetlana Tessalina
John de Laeter Centre, Curtin University, WA 6102
svetlana.tessalina@curtin.edu.au

Lena Hancock
Geological Survey of Western Australia DMIRS, East Perth, WA 6004
Lena.HANCOCK@dmirs.wa.gov.au

Bryant Ware
John de Laeter Centre, Curtin University, WA 6102
bryant.ware@curtin.edu.au

Neal McNaughton
John de Laeter Centre, Curtin University, WA 6102
N.McNaughton@curtin.edu.au

Laure Martin
CMCA, University of Western Australia M010, Perth WA 6009
laure.martin@uwa.edu.au

SUMMARY

Characterisation of the source of hydrothermal gold deposits typically relies on isotopic composition and textural interpretations of co-precipitating minerals. However, native gold contains trace elements and mineral inclusions of value to source characterisation. In this work, we studied several small gold nuggets from placer occurences in the Kurnalpi Terrane, Yilgarn Craton, Western Australia for their geochemical and isotopic characteristics using thermal ionisation mass spectrometry (TIMS) and secondary ion mass spectrometry (SIMS) methods. One of the most important findings of this study was the establishment of reliable Pb-Pb model ages for some gold samples, as well as the characterisation of the source of Pb prior to mineralisation. We establish that galena inclusions in native gold preserve Pb-isotope compositions compatible with known Archean deposits in the Kurnalpi Terrane, and that some native gold grains contain <10 ppm Pb and virtually exclude U, allowing initial Pb-isotope compositions to be measured. This study demonstrates that the geochemical and isotopic fingerprints of native gold could be used for exploration of primary gold sources, and potentially identify transport corridors.

Key words: gold, nugget, placer, fingerprinting, Pb isotopes

INTRODUCTION

The recent Curtin-GSWA geochemical-isotopic collaborative study of small gold nuggets from WA placer gold occurences and deposits (Tessalina et al., *in press*) has demonstrated our analytical capability to produce a coherent set of trace element and isotope data to fingerprint native gold. In our study, we investigated several gold nuggets from the Kurnalpi Terrane in the Archean Yilgarn Craton (among other locations in Western Australia) with the aim to establish the age and constrain the source of gold mineralisation directly from gold. The samples were analysed for Pb isotopes, PGEs, REEs and other trace elements.

GEOLOGICAL SETTING AND SAMPLE LOCATION

Placer gold nuggets for this study were sourced from gravels beneath the surface from an 80 km^2 area of the Archean Kurnalpi Terrane in the Eastern Goldfields Superterrane, Yilgarn Craton, located about 85 km east-northeast of Kalgoorlie. Local bedrock consists of metamorphosed basalt aged 2960–2650 Ma, with dolerite-textured zones and feldspar-hornblende or chlorite schist.

No operating gold mines occur in the area. Known sub-economic bedrock-hosted gold mineralization appears to have been the greenstone-hosted orogenic style. It occurs in quartz veins with microscopic gold and associated silica–pyrite ± carbonate ± hematite alteration in metabasalt, and magnetite-bearing, granophyric quartz dolerite dykes that cut ultramafic rocks (Hancock and Beardsmore, 2020).

This study uses several placer gold nuggets collected from thin gravels at the base of Quaternary channels buried 1–2 m beneath surficial loam, and from Cenozoic laterite and calcrete deposits and buried paleochannels. There are up to 40 m of detrital zones in the Cenozoic regolith that preserved the history of weathering, erosion and landscape development. In addition, the Yilgarn Craton was extensively glaciated during the early Permian and was at least locally incised by subglacial channels.

The selected gold nuggets (Fig. 1) show various degrees of alteration and recrystallization, from mono-crystalline to mostly recrystallized microstructure, often with polysynthetic twinning and Ag-free veinlets and Ag-depleted porous zones in external rims. The nuggets are slightly- to well-rounded (Fig. 1) with smooth and spongy surfaces and have both primary (quartz, tellurides, galena) and secondary (maghemite) mineral inclusions. Two nuggets studied contain galena micro-inclusions.

METHODS

Pb-Pb isotope analysis

TIMS

The Pb content in native gold is generally too low for a precise Pb isotope measurement by an *in-situ* analytical methods (e.g., Laser Ablation-Inductively Coupled Plasma-Mass Spectrometry, SIMS). Accordingly, sufficient sample of native gold was taken and dissolved in acids, and the Pb extracted by conventional ion exchange chromatography for TIMS analysis. To yield sufficient Pb for analysis ~100 mg of gold was generally required: smaller sample amounts generally gave less precise Pb isotope ratios.

To avoid contamination from sampling, the recovered gold samples were acid washed in 50% HCl in an ultrasonic bath, rinsed and ultrasonically cleaned several times in distilled water, and then dried in a clean hood. The *aqua regia* acid digestion was carried out using concentrated acids (3 ml of purged double-distilled HNO_3 and 1 ml of triple distilled HCl). Digestion of samples was done using two different methods: (1) the first batch of samples (separated by dental drill) with smaller amounts available (2 to 10 mg) was digested in Teflon bombs in the oven at 140ºC; (2) the second batch (separated by hand drill) with larger amounts of material available, was digested in Pyrex™ borosilicate Carius tubes and heated to 220°C for 36 hrs. Accurate and precise measurements of Pb isotope compositions were made using TIMS Triton™; trace elements abundances were measured in solution mode using Element™ HR-ICPMS.

SIMS

To compare the Pb isotope signatures recorded in gold and its Pb-rich inclusions (galena and hessite [Ag_2Te]), in-situ analysis of Pb isotopes by SIMS were conducted in two gold samples using a Cameca IMS1280 equipped with a high-brightness Oregon Physics Hyperion-II RF-plasma oxygen ion source hosted at CMCA-UWA.

Gold samples were mounted in epoxy, polished flat using mechanical polisher and diamond suspension liquids, and then ion milled. Prior to SIMS analyses, mounts were cleaned with ethanol, deionised water, and a ~10 nm gold coating was applied. For Pb isotopes in galena and hessite, a mass filtered, 200pA $^{16}O_2^-$ primary ion beam was focused in Gaussian mode and rastered over a 15x15mm area. A larger 25 x 25 mm area was pre-sputtered for 120s to remove the coating gold and clean the surface from potential surficial contamination. This procedure was followed by automatic centring of the secondary ion beam within the 4000 µm field aperture and optimisation of mass calibration, performed automatically for each run using $^{208}Pb^+$. Entrance and exit slits were set to 122µm and 300µm, respectively, to achieve a mass resolving power of ~4000. Secondary ions ^{202}Hg, ^{204}Pb, ^{206}Pb, ^{207}Pb and ^{208}Pb were collected in the axial ETP electron multiplier (EM), in monocollection mode by switching the magnetic field to acquire the different masses. Typical count rates for $^{208}Pb^+$ in galena using a 200pA ion beam is $1.8x10^5$ cps. ^{202}Hg, ^{204}Pb, ^{206}Pb, ^{207}Pb and ^{208}Pb were counted for 8s, 8s, 3s, 3s and 2s, respectively, during 20 cycles. Possible isobaric interference of ^{204}Hg on ^{204}Pb was monitored using ^{202}Hg but found negligable (<0.001%). Accuracy of Pb isotope data was checked on (i) a USGS-BCR2 glass (Woodhead et al., 2007), and (ii) a set of galena crystals with known Pb isotope composition. The consistency for both glass and galena samples between TIMS or published data and SIMS measured average values demonstrated the absence of a significant instrumental mass fractionation during these measurements.

For Pb isotope measurements of gold, a 15nA $^{16}O_2^-$ primary ion beam was rastered over a 15x15mm area after a pre-sputtering over a 25x25 mm area for 120s. At the beginning of each analysis, the secondary ion beam was centred within the 5000 µm field aperture and mass calibration was performed using ^{197}Au. Entrance and exit slits were set to 243µm and 300µm, respectively, to achieve a mass resolving power of ~4000 while optimising Pb^+ transmission through the mass spectrometer. Secondary ions ^{197}Au, ^{202}Hg, ^{204}Pb, 204.3, ^{206}Pb, ^{207}Pb and ^{208}Pb were collected in the axial EM in monocollection mode. Typical count rate for $^{208}Pb^+$ in gold using a 15nA ion beam is <100 cps. ^{202}Hg, ^{204}Pb, 204.3, ^{206}Pb, ^{207}Pb and ^{208}Pb were counted for 8s, 8s, 4s, 3s, 3s and 2s, respectively, during 40 cycles. Isobaric interference of ^{204}Hg on ^{204}Pb was corrected using ^{202}Hg and the natural abundance of ^{204}Hg and ^{202}Hg isotopes. Background correction on axial EM was performed using intensities measured on the 204.3 mass.

Trace elements

An aliquot of sample solution removed from the reverse *aqua regia* solution was used for trace element analyses and to perform quality checks on procedural and analytical processes. The aliquot was evaporated and redigested into diluted nitric acid for ICPMS analyses. Two different dilutions were made for trace element determination: a high concentration solution was created for measurement of rare earth elements (REEs), and a lower concentration (more diluted) solution was created for measurement of high-concentration elements in Au (e.g. Ti, Cu, Zi, Pb, etc.). Trace element concentrations were acquired using an Element™ HR-ICPMS. After signal and instrument optimization was obtained using a 1 ng g^{-1} tuning solution, measurements of trace elements and REEs were performed in low resolution to obtain the highest sensitivity available due to the low REE contents of native gold. All elements were analysed in triple-counting mode to allow the determination of higher-concentration elements by analogue counting or on the Faraday detector at the same time as determining lower-concentration elements (e.g. REEs) by pulse counting. Concentrations were determined via the relationship between the unknowns and a set of prepared standard solutions. Mixed standard solutions of different concentrations of the desired elements used for external concentration determinations were analysed after about every 10 unknowns. To monitor quality and potential memory effects, acid blanks were measured at regular intervals throughout the analytical sessions. To compensate for instrumental mass drift, the mass offset and automatic mass lock features of the ThermoFisher Element™ software were utilized in conjunction with each analytical blank being spiked with 1 ppb of In as an internal standard. An assessment of accuracy of the high-concentration elements in Au results was conducted using three Reference Materials for native Au. [Svet: you don't mention PGEs, but Pd is plotted in Fig. 3. For PGEs, did you use ID? If so, you should add a sentence in this section].

RESULTS

Pb-Pb isotope systematics

Galena inclusions analysed by both TIMS and SIMS methods display the most primitive Pb isotopic composition ranging from 13.53 to 13.55 for $^{206}Pb/^{204}Pb$ ratio (Fig. 2, samples 201941 and 201943) with Neoarchean model ages of 2.65-2.66 Ga according to the best fit lead growth model (Abitibi-Wawa; Huston et al., 2014). The Pb-rich hessite inclusion in gold from the sample 201946 displays slightly more radiogenic Pb composition with $^{206}Pb/^{204}Pb$=13.753 and $^{207}Pb/^{204}Pb$=14.919, with higher model source μ value of 8.8 ($\mu = {}^{238}U/^{204}Pb$).

Gold nuggets contain slightly more radiogenic Pb than galena. For example, native gold from sample 201943 analysed by TIMS is 0.5% more radiogenic than galena inclusions in the same nugget ($^{206}Pb/^{204}Pb$ ranges from 13.59 to 13.61 for two duplicates), despite containing only 3.5-7.8 ppm Pb. Partly recrystallized gold from sample 201941 analysed by SIMS displays slightly more radiogenic Pb isotope composition than galena inclusions, with $^{206}Pb/^{204}Pb$ ratio of 13.97.

Sample 201954 without visible galena inclusions also displays a more radiogenic Pb isotope composition of 13.82 for $^{206}Pb/^{204}Pb$ with a younger Pb model age of 2.44 Ga. This reflects minor radiogenic Pb addition during gold burial alteration and demonstrates that native gold may preserve both the initial Pb and later, more radiogenic, Pb.

However, together with primitive Neoarchean Pb isotope compositions, some gold nuggets display highly radiogenic Pb isotope ratios up to 17.8 for $^{206}Pb/^{204}Pb$ (close to present-day Bulk Silicate Earth estimate) as detected in two samples (Fig. 2; samples 201929 and 201930). This near-zero model age for Pb would possibly reflect the age of the regolith, ranging from 52 to 0 Ma for oxides (Dammer et al., 1999), as dated using K-Ar and ^{40}Ar-^{39}Ar methods. Both of these samples have elevated Pb-contents and are characterized by elevated trace elements, especially for Cu and Zn, which may signify the input of trace elements, including more radiogenic Pb, during alteration processes of nuggets throughout their transport/burial history.

Trace elements

Selected trace element plots are presented in Figure 3. In the analyzed solutions of Kurnalpi gold nuggets, median trace element abundances decrease in the following order (in ppm): Cu [623] → As [54] → Zn [18] → V [15] → Ti [8] → Ni [2] → Pb [2] → Mn [0.5] → Co [0.1] → Cd [0.1] → Bi [0.04] → U [0.006]. The samples with highest Cu and Zn contents also have the highest Pd, Ni and Pb, which suggests an association between these elements. The correlation coefficients calculated for Cu decrease in the following order: Cu → Pd → Zn → Pb → Pt (0.90 → 0.86 → 0.85 → 0.65 respectively). For Pb, a similar range has been calculated: Pb → Zn → Ni → Pd → Cu (0.99 → 0.93 → 0.90 → 0.85 respectively). The overall slope and REE contents are similar to or lower than those for ore-hosting andesite from the Kurnalpi Terrane (Park and Campbell, 2020). The enrichment in light REE is pronounced, with a slight Ce anomaly presented in some samples.

DISCUSSION

Galena inclusions in gold display the most primitive Pb isotopic composition with Neoarchean model ages ranging from 2.65-2.66 Ga. These model ages correspond to the main mineralization events in the area, such as ca. 2.64 Ga gold mineralization event in the Eastern Goldfields (Vielreicher et al., 2015), that is slightly younger than stratiform 2.7 Ga VHMS mineralization in the Kurnalpi Terrane.

To investigate the sources of Pb in native gold, we refer to the better-known stratiform VHMS deposits from the same area, formed around 2.7 Ga (e.g., Barrote et al., 2020a). The initial Pb for two VHMS deposits (Teutonic Bore and Nimbus) are shown on Figure 2. The Teutonic Bore deposit belongs to the Teutonic Bore camp located within the Kurnalpi terrain and is the most relevant to this study (e.g., Barrote et al., 2020b). Nimbus VHMS deposit is situated near the margin between the Kalgoorlie and Kurnalpi Terranes (Barrote et al., 2020a). The Teutonic Bore deposit displays the most primitive Pb isotope composition with the most primitive model source μ-value ($^{238}U/^{204}Pb$) of 8.1 (re-calculated after McNaughton et al., 1990). This low μ-value is consistent with S isotopic composition of ore sulphides being mainly of mantle origin ($\delta^{34}S$ = − 0.83 to + 1.89‰; $\Delta^{33}S$ = − 0.46 to − 0.05 ‰) and distinct from sedimentary sulphides ($\delta^{34}S$ = + 0.88 to + 14.86‰; $\Delta^{33}S$ = + 0.19 to + 6.20‰) both locally and regionally (Chen et al., 2015). Chen et al. (2015) suggested the mantle S is likely to be derived from a magmatic-hydrothermal fluid, rather than from magmatic sulphides in the footwall volcanic rocks by leaching. The Nimbus deposit displays a higher model source μ-value of 8.4. High-grade Zn-Ag mineralization from Nimbus deposit was interpreted as having predominantly a magmatic sulphur source (Caruso et al., 2018) as supported by sulphur isotope signatures sourcing sulphur and fluids largely from a magmatic reservoir ($\Delta^{33}S$ = +0.09%).

Epigenetic gold deposits from Norseman-Wiluna Belt are also shown for comparison (Fig. 2B). The apparent heterogeneity in initial Pb isotopic composition among epigenetic gold deposits in this area was explained by the crustal contamination of mantle-derived fluids (McNaughton et al., 1990). The 2.7 Ga mixing line in Figure 2A represents the mixing between a greenstone and mantle Pb reservoir (represented by Teutonic Bore) and an older, enriched in U/Pb, crustal reservoir. This comparison demonstrates that the initial Pb for the gold deposits in the Terrane was variable, and different nuggets may be from different sources and not have the same initial Pb at the time of formation. The source μ ($^{238}U/^{204}Pb$) values for less radiogenic galena inclusions in gold (8.17 to 8.28) are similar to values of volcanogenic massive sulphide deposits Teutonic Bore ($^{238}U/^{204}Pb$=8.1) and Nimbus ($^{238}U/^{204}Pb$=8.4), indicating mostly a juvenile, predominantly mantle-derived source of Pb. The more radiogenic compositions from native gold could reflect an Archean nugget with a more radiogenic initial Pb than the galena inclusions and either in-situ U-decay within in the nugget, and/or a more complex history including Pb mobilisation, particularly at younger times. The Pb isotope composition of some of the placer native gold nuggets was affected by post-formation processes, probably in more recent times such as burial in a regolith. The chemical/isotopic fingerprint of gold from documented orebodies, for comparison purposes, has yet to be addressed.

CONCLUSIONS

One of the most important results was establishing reliable Pb–Pb model ages for some gold samples, as well as characterizing the source of Pb prior to mineralization. For the Kurnalpi Terrane, the results indicate that the nuggets are of similar age and composition to known bedrock mineralization in the region, implying a common age and origin. Galena inclusions in gold nuggets from the Kurnalpi Terrane display the most primitive Pb isotope compositions, with Neoarchean model ages ranging from 2.72 to 2.65 Ga, similar to ages of the host rocks. The source μ ($^{238}U/^{204}Pb$) values for galena inclusions and less-altered gold nuggets from the Kurnalpi Terrane range from 8.17 to 8.28, similar to values for volcanogenic massive sulfide deposits at Teutonic Bore and Nimbus (8.1 and 8.4, respectively). These results indicate a mostly juvenile, predominantly mantle-derived source for Pb.

REFERENCES

Hancock, E.A., and Beardsmore, T.J., 2020, Provenance fingerprinting of gold from the Kurnalpi Goldfield: Geological Survey of Western Australia, Report 212, 21p.

Barrote, V.R., Tessalina, S.G., McNaughton, N.J., Jourdan, F., Hollis, S.P., Ware, B. and Zi J.-W., 2020a, 4D history of the Nimbus VHMS ore deposit in the Yilgarn Craton, Western Australia: Precambrian Research, 337: 105536.

Barrote, V.R., McNaughton, N.J., Tessalina, S.G., Evans, N.J., Talavera, C., Zi J.-W., and McDonald B.J. 2020b, The 4D evolution of the Teutonic Bore Camp VHMS deposits, Yilgarn Craton, Western Australia: Ore Geology Reviews 120: 103448.

Caruso, S., Fiorentini, M.L., Hollis, S.P., LaFlamme, C., Baumgartner, R.J., Steadman, J.A., and Savard D., 2018, The fluid evolution of the Nimbus Ag-Zn-(Au) deposit: An interplay between mantle plume and microbial activity: Precambrian Research, 317, 211–229.

Chen, M., Campbell, I.H., Xue, Y., Tian, W., Ireland, T.R., Holden, P., Cas, R.A.F., Hayman, P.C., and Das, R., 2015, Multiple sulfur isotope analyses support a magmatic model for the volcanogenic massive sulfide deposits of the Teutonic Bore volcanic complex, Yilgarn Craton, Western Australia: Economic Geology, 110(6): 1411.

Dammer, D., McDougall, I., and Chivas, A.R., 1999, Timing of Weathering-Induced Alteration of Manganese Deposits in Western Australia: Evidence from K/Ar and 40Ar/39Ar Dating: Economic Geology, 94, 87–108.

Huston, D.L., Champion, D.C., and Cassidy, K.F., 2014. Tectonic controls on the Endowment of Neoarchean Cratons on volcanic-hosted massive sulphide dedposits: evidence from Lead and Neodymium isotopes. Economic Geology, 109, 11-26.

Maltese, A., and Mezger, K., 2020, The Pb isotope evolution of Bulk Silicate Earth: Constraints from its accretion and early differentiation history: Geochimica et Cosmochimica Acta, 271, 179–193.

McNaughton, N.J., Cassidy, K.F., Dahl, N., Groves, D.I., Perring, C.S., and Sang, J.H., 1990, Lead isotope studies. In: Susan, EH, Groves, DI and Bennett, JM (Ed) Gold deposits of the Archaean Yilgarn block, Western Australia: Nature, Genesis and Exploration guides, UWA publication 20, 226–236.

Park, J.-W., and Campbell, I., 2020, Platinum-group element geochemistry of the volcanic rocks associated with the Jaguar and Bentley Cu–Zn volcanogenic massive sulfide (VMS) deposits, Western Australia: implications for the role of chalcophile element fertility on VMS mineralization: Mineralium Deposita, https://doi.org/10.1007/s00126-020-00991-9.

Tessalina et al. in prep. Isotopic fingerprinting of native gold from Western Australia. GSWA report.

Vielreicher, N.M., Groves, D.I., McNaughton, N.J., and Fletcher, I.R., 2015, The timing of gold mineralization across the eastern Yilgarn craton using U–Pb geochronology of hydrothermal phosphate minerals: Mineralium Deposita, 50, 391–428.

Figures

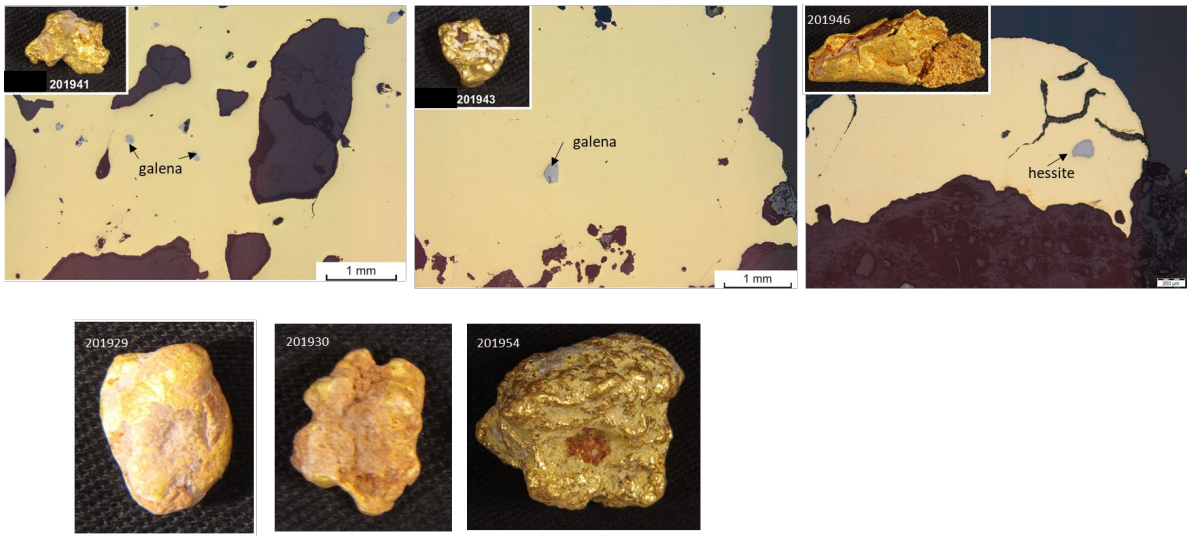

Figure 1. Gold nuggets, some with galena and hessite inclusions, selected for isotope and trace element analysis. [Svet: scale bars???]

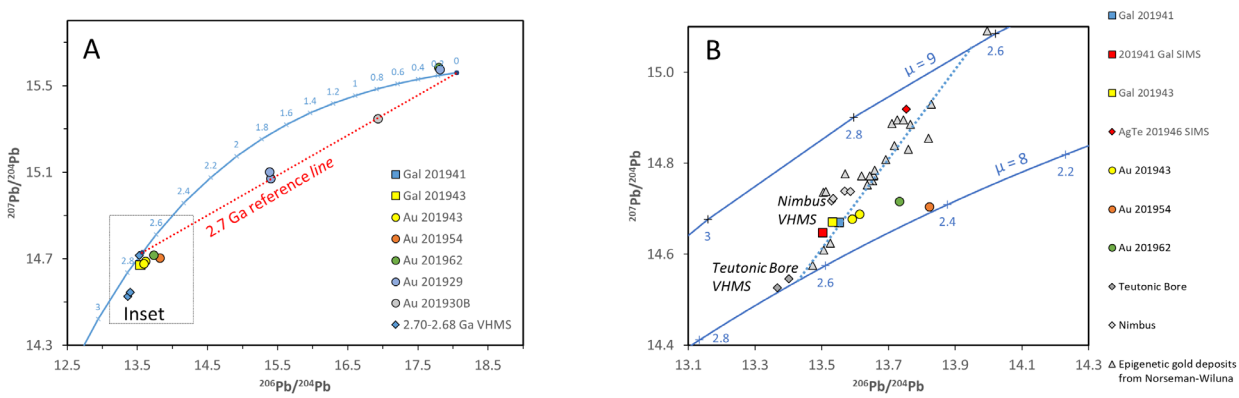

Figure 2. (A) $^{206}Pb/^{204}Pb$ versus $^{207}Pb/^{204}Pb$ plot for galena and native gold from the Kurnalpi Terrane. Lead growth curve (Maltese and Mezger, 2020). Volcanic-Hosted Massive Sulphide (VHMS) deposits Nimbus (Barrote et al., 2020a) and Teutonic Bore (Barrote et al., 2020b) are shown for comparison. (B) $^{206}Pb/^{204}Pb$ versus $^{207}Pb/^{204}Pb$ plot for galena and native gold from Kurnalpi Terrane, in comparison with VHMS deposits and epigenetic gold mineralisation from Norsman-Wiluna Terrane (McNaughton et al., 1990). Lead growth curve with two different μ values ($^{238}U/^{204}Pb$) are shown. Note that deposits are distributed along the line depicting similar age but different μ values, reflecting mixture between more juvenile (e.g., Teutonic Bore) and more "crustal" sources.

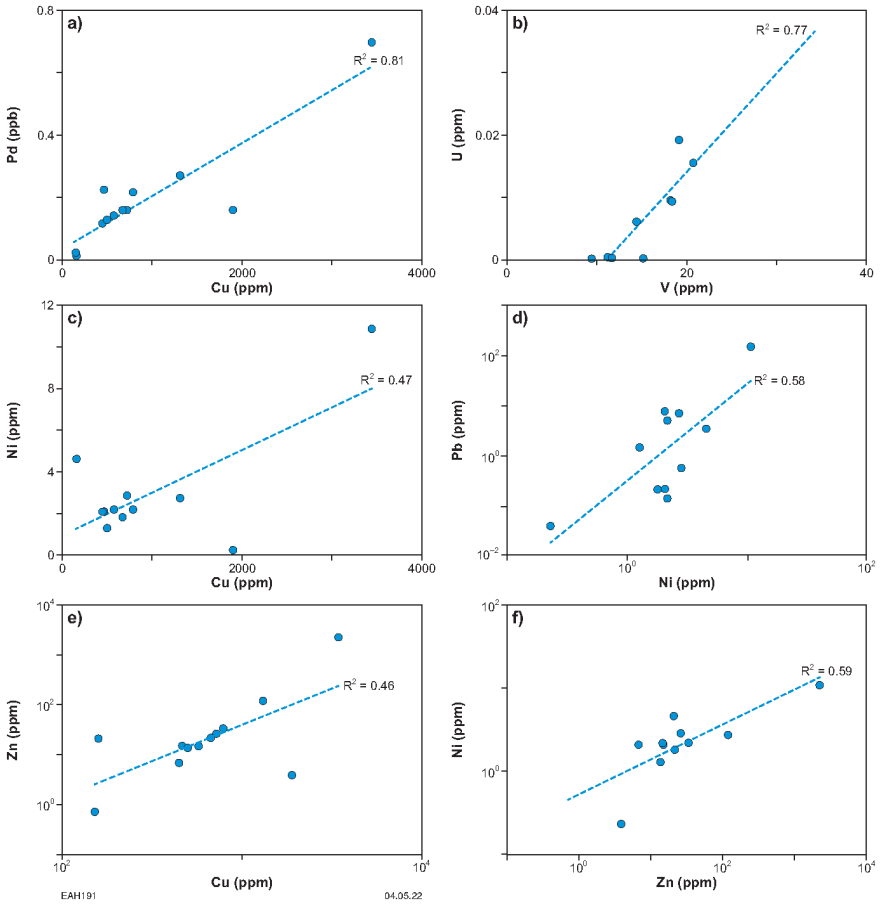

Figure 3. Trace element concentrations in native gold nuggets from the Kurnalpi Terrane: a) Cu vs Pd; b) V vs U; c) Cu vs Ni; d) Ni vs Pb; e) Cu vs Zn; f) Zn vs Ni.